*Desalination and Water Treatment*
www.deswater.com
doi: 10.5004/dwt.2020.24986

179 (2020) 387–395
March

# In-situ synthesis of hydrogen peroxide using water electrolysis and Pd/MWCNTs catalyst

Shunxi Zhang[a,b,*], Zhen Yue[b], Xiaofeng Pang[b], Mengzhen Pan[b], Jingjing Tang[b], Xianzhong Cheng[b], Jianfen Li[b,*], Yulan Liu[a], Wenjuan Shen[b]

[a]*Hubei Key Laboratory of Animal Nutrition and Feed Science, Wuhan Polytechnic University, Wuhan, 430023 Hubei, China, Tel. +86 15307133273; Fax: +86 27 83956762; emails: shunxizhang@163.com (S.X. Zhang), 934887324@qq.com (Y.L. Liu)*
[b]*Department of Chemical and Environmental Engineering, Wuhan Polytechnic University, Wuhan, 430023 Hubei, China, emails: 405360494@qq.com (J.F. Li), 2939315308@qq.com (Z. Yue), 782054337@qq.com (X.F. Pang), 1114691869@qq.com (M.Z. Pan), 1531547292@qq.com (J.J. Tang), 190474202@qq.com (X.Z. Cheng), 1025009469@qq.com (W.J. Shen)*

Received 25 April 2019; Accepted 30 September 2019

**ABSTRACT**

At room temperature and atmospheric pressure, water electrolysis and Pd/MWCNTs catalyst are used to investigate the feasibility of in-situ synthesizing hydrogen peroxide in a safe way. Meantime, the ordinary Ti/β-$PbO_2$ anode and graphite cathode are adopted to construct the water electrolysis system. During experiments, the features of Pd/MWCNTs catalyst are characterized by transmission electron microscope/energy dispersive spectrometer, X-ray diffraction and X-ray photoelectron spectroscopy. The effect of pH, current density, catalyst dosage, interelectrode distance, agitation speed and different cations on $H_2O_2$ concentration is studied. Energy consumption for different current density is analyzed, too. The results show that $H_2O_2$ concentration for the optimal conditions, namely current density of 20 mA/cm$^2$, pH of 3, catalyst dosage of 0.5 g, interelectrode distance of 20 mm and agitation speed of 460 rpm, can attain to about 28 mg/L in 90 min. Additionally, under the above conditions, $H_2O_2$ concentration for water including $Mg^{2+}$ ion can rapidly get to about 36 mg/L in 30 min. $E_m$ increases from 213.0 to 368.8 kWh/kg when current density varying from 10 to 25 mA/cm$^2$. However, for the lowest current density of 5 mA/cm$^2$, its $E_m$ is 288.5 kWh/kg and is very high, too. The used process is feasible for in-situ synthesis of hydrogen peroxide.

*Keywords:* Hydrogen peroxide; Pd/MWCNTs catalyst; Ti/β-$PbO_2$ anode; In-situ synthesis; Water electrolysis

## 1. Introduction

Hydrogen peroxide ($H_2O_2$) is one of the most important chemical materials and is widely used in various fields, such as wastewater treatment, pulp and paper industry, cosmetic and pharmaceutical industry, chemical synthesis, semiconductor cleaning and soil remediation [1–8]. Thereinto, due to powerful and environmentalfriendly characteristic, the demand for hydrogen peroxide in wastewater treatment is becoming more enormous, specially the Fenton oxidation process spurting. However, at present, hydrogen peroxide is mainly produced by anthraquinone autooxidation process, which has a relatively high cost and easily brings environmental hazards [1–3,9–15]. In addition, during the transportation and storage of concentrated peroxide solution, special precaution related to safety needs to be considered [1–3,9–15]. Moreover, for the typical end consumers, the concentrated $H_2O_2$ for reducing transportation cost is generally diluted to a concentration of 2–8 wt.% for use [5,16,17].

* Corresponding authors.

Consequently, to meet the consumers' requirements and avoid the environmental and safe risks, the low cost, small scale and on-site processes about hydrogen peroxide production have attracted the researchers' concerns [14,15,17–20]. Typically, direct synthesis of hydrogen peroxide utilizing hydrogen and oxygen is considered as one of the promising processes due to its economical and environmentally benign features [4,8,19,21].

Currently, during direct synthesis of hydrogen peroxide, hydrogen and oxygen are used directly as raw materials. Because of the low solubility of oxygen and hydrogen in water, high pressure up to over 100 bar is generally adopted in order to further increase the yield [1,16]. Additionally, the reactions involved in the direct synthesis of hydrogen peroxide are as below [1,3,4,7,10].

Oxidation of hydrogen to hydrogen peroxide:

$$H_2 + O_2 \rightarrow H_2O_2 \quad (1)$$

Formation of water:

$$2H_2 + O_2 \rightarrow 2H_2O \quad (2)$$

Decomposition of hydrogen peroxide:

$$2H_2O_2 \rightarrow 2H_2O + O_2 \quad (3)$$

Hydrogenation of hydrogen peroxide:

$$H_2O_2 + H_2 \rightarrow 2H_2O \quad (4)$$

According to Eqs. (1)–(4), the undesired reactions of Eqs. (2)–(4) also emerge together with the main synthesis reaction of Eq. (1). For this reason, the palladium–based catalysts, such as Pd, Pd-alloy and bimetallic Au–Pd catalyst [1–26], are widely applied to obtain high yield and selectivity of hydrogen peroxide [1,3,4,6,13,16]. Meantime, for the effective distribution of active components, palladium is ordinarily supported on some porous materials such as $SiO_2$, $TiO_2$, $Al_2O_3$, and activated carbon [1–26]. However, when hydrogen and oxygen are directly supplied, due to a broad explosive range of $H_2/O_2$ mixtures, the safe challenge must be faced during the direct synthesis of hydrogen peroxide. Furthermore, in some processes, high pressure is adopted to enhance the yield [1,16], which further increases the safety risk. For that, to reduce the explosive potential, hydrogen and oxygen generated from water electrolysis are directly adopted by a few researchers to in-situ synthesis of hydrogen peroxide [20]. However, the noble metal electrodes, such as Pt, are often utilized [20], which prevents the process spreading in wastewater treatment field. Additionally, the support materials for catalyst are required to have highly settleable performance, as is favorable to recovery and reuse of catalyst. To this end, the researchers are trying their best to make the above process better so that it can be used in wastewater treatment in a safe way.

The anode of Ti/β-$PbO_2$, owing to stable physical and chemical features, easy preparation and low cost, is widely used for pollutant removalfrom wastewater [27,28]. In addition, multi-walled carbon nanotubes (MWCNTs) are very fluffy and can be dispersed rapidly into water by mechanical stirring. Meantime, it is found that MWCNTs have highly settleable feature in water and can settle down quickly to achieve solid-liquid separation. Consequently, we think that MWCNTs are a very suitable support material for catalyst when the in-situ synthesizing hydrogen peroxide is applied in wastewater treatment. However, during in-situ synthesis of hydrogen peroxide, the Ti/β-$PbO_2$ anode and the MWCNTs support material for catalyst are used, which is seldom reported up to now.

In this paper, the ordinary Ti/β-$PbO_2$ anode and graphite cathode are used to construct the water electrolysis system. At room temperature and atmospheric pressure, water electrolysis and Pd/MWCNTs catalyst are adopted to realize in-situ synthesis of hydrogen peroxide in a safe way. During the experiments, the features of Pd/MWCNT catalyst are characterized by transmission electron microscope (TEM)/energy dispersive spectrometer (EDS), X-ray diffraction (XRD) and X-ray photoelectron spectroscopy (XPS). Next, the effect of pH, current density, catalyst dosage, interelectrode distance, agitation speed and different cations on $H_2O_2$ concentration is investigated. Finally, energy consumption for different current density is analyzed. The aims of this paper are to demonstrate the feasibility of in-situ synthesizing hydrogen peroxide using water electrolysis and Pd/MWCNTs catalyst. Additionally, the work will bring a new production method of hydrogen peroxide applied to wastewater treatment in a safe way.

## 2. Materials and methods

### 2.1. Preparation of Pd/MWCNTs catalyst

Palladium acetate of 0.105 g, which is purchased from Shanxi Kaida Chemical Reagent Co. Ltd., China, is dissolved in 6 mL HCl solution of 1 mol/L at 60°C. After that, the above mixture is oxidized by addition of 2 mL solution (10%NaClO:10%$H_2O_2$ = 1:5) for 5 min. Next, the mixture is dumped slowly into 1 g MWCNTs which are of industrial grade and supplied by Suzhou Tanfeng Techology Inc., China. Then, the slurry is mixed by ultrasonic vibration for 10 min. Thereafter, 20 mL sodium formate solution of 3 mol/L is added into the slurry. Finally, the slurry, which is kept still for 4 h at 70°C, is washed by distilled water and sent to dry at 60°C under vacuum. Through the above operations, Pd/MWCNTs catalyst with the predetermined Pd loading of 5 wt.% is obtained.

### 2.2. Experimental setup and procedure

The experimental setup is schematically demonstrated in Fig. 1. Prior to a test, a given mass catalyst of Pd/MWCNTs is put into a glass beaker with a magnetic rotor. Next, 100 mL of the prepared solution containing 0.1 mol/L $Na_2SO_4$ is dumped into the above beaker. Then, the Ti/β-$PbO_2$ anode and graphite cathode are parallel inserted into the solution to a depth of 50 mm, and then the magnetic agitator is run at a given agitation speed. Finally, the DC power, which is purchased from Shenzhen Zhaoxin Electronic Instrument

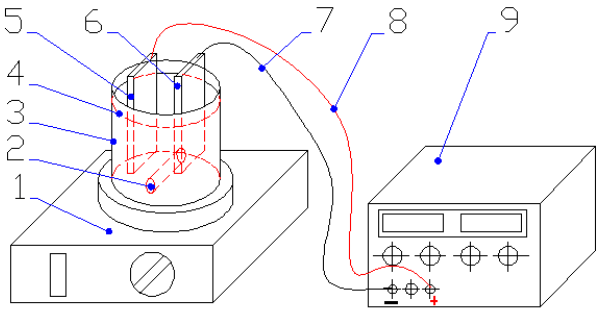


Fig. 1. Diagram of the experimental setup. (1) Magnetic agitator, (2) magnetic rotor, (3) glass beaker, (4) water surface curve, (5) Ti/β-$PbO_2$ anode, (6) graphite cathode, (7) negative wire, (8) positive wire, (9) DC power.

Equipment Co. Ltd., China, is connected to the electrodes and operated in a constant current mode. Meantime, a timer is turned on to record reactive time.

Before a run, the solution is prepared by addition of $Na_2SO_4$ into distilled water to improve its conductivity. Simultaneously, pH value is adjusted by addition of 1 mol/L $H_2SO_4$ according to the experimental demand. During the experiments, the adopted Ti/β-$PbO_2$ anode is home-made by the electrodepositing method according to literatures [27,28], and its size is 75 × 20 × 1 mm. The used graphite cathode with the dimension 75 × 25 × 1 mm is of high purity (≥99.5%) and bought from Beijing Crystal Special Carbon Technology Co. Ltd., China.

During each run, the sample of 6 mL is taken at a desired time. Thereafter, the prepared solution of 6 mL is supplemented immediately into the beaker, and the above operation is repeated until the test is finished. Next, the sample is centrifuged at 4,000 rpm for 5 min, and then the supernatant is filtered by a sand core filtration unit with a micro-porous membrane. Finally, the filtrate is sent to analyze physical–chemical parameters. Pd/MWCNTs catalyst settled by centrifugation is rinsed by distilled water into a plastic centrifugal tube of 100 ml. In addition, when the trial is finished, the residual solution is also dumped into the above tube and centrifuged at 3,000 rpm for 10 min. At last, Pd/MWCNTs catalyst settled in the tube is air-dried for future trials.

### 2.3. Analytical methods

The content of $H_2O_2$ produced in the solution is measured at 405 nm by a spectrophotometer (Unico 7200, Unicol [Shanghai] Scientific Instrument Co. Ltd., China) after coloration with $TiSO_4$ [20]. pH value is determined with a pH meter (Hach 2000, Hach Company, USA). Conductivity is monitored by a conductivity meter (DDS-11C, INESA Scientific Instrument Co. Ltd., Shanghai, China).

The features of Pd/MWCNTs catalyst are characterized by X-ray diffraction (XRD-7000, SHIMADZU, Japan), TEM (; FEI Tecnai G2 F30 S-TWIN, FEI, USA) coupled with an energy dispersive spectrometer (EDS) and X-ray photoelectron spectroscopy (XPS) (PHI 5000 VersaProbe, ULVAC-PHI, Japan).

## 3. Results and discussion

### 3.1. Characterization of Pd/MWCNTs catalyst

The TEM image of the fresh Pd/MWCNTs catalyst (Fig. 2) shows that some small particles with the size of 5–13 nm (mean size 8.1 nm in the histogram) are homogeneously dispersed on the surface of MWCNTs. Simultaneously, the small particles are identified as Pd particles according to the results of EDS and its content is about 1.4 wt.%. However, the TEM image of the used catalyst reveals that the Pd particles are partly aggregated with particle size about 5–17 nm (mean size 11.4 nm in the histogram) and the content decreases to about 1.2 wt.%.

The XRD patterns of the used and fresh Pd/MWCNTs catalysts (Fig. 3) all demonstrate the existence of Pd. Thereinto, the five diffraction peaks at 40.3°, 46.7°, 68.4°, 82.3° and 86.9° represent, respectively, the (111), (200), (220), (311) and (222) planes of Pd, which infer that Pd exists in the form of the typical face-centered cubic (FCC) crystal structure [29–35]. According to the Debye–Scherrer formula [33], the average crystalline sizes of the fresh and used catalysts are 8.3 and 11.1 nm, respectively, which is in general accord with the results from the TEM.

XPS demonstrates that there are two sets of 3d peaks in the $Pd_{3d}$ core spectrum of the fresh Pd/MWCNTs catalyst (Fig. 4). Thereinto, the one set including Pd3d3/2 (342.9 eV) and Pd3d5/2 (337.7 eV), namely Pd(II) species, can be designated as PdO and $PdO_2$, respectively. Similarly, the other set containing Pd3d3/2 (340.9 eV) and Pd3d5/2 (335.8 eV), namely Pd(0) species, can be assigned to Pd metal, which are in accord with the literatures [31,32,34,35]. Additionally, the XPS quantitative analysis shows that the contents of Pd and MWCNTs are 1.12 wt.% and 93.51 wt.%, respectively.

### 3.2. Influential factors

#### 3.2.1. Effect of pH

pH value of water body is a vital parameter and generally influences on the characteristics of water electrolysis and catalyst. Fig. 5 shows the effect of pH on $H_2O_2$ concentration.

Seen from Fig. 5, $H_2O_2$ concentrations for pH 1 and 2 all climb rapidly to a top in 30 min and then slightly decrease. Similarly, $H_2O_2$ concentrations for pH 4 and 5 increase to a high point in 15 min and then are in a slight fluctuation state. However, for pH 3, $H_2O_2$ concentration seemingly improves in a straight way and attains to the highest value of 16 mg/L in 120 min. At the same time, it is noted that $H_2O_2$ concentration for pH 7 is very little and is almost zero except for 15 and 120 min. In addition, it is found that at the same instant $H_2O_2$ concentrations decrease when pH changes from 3 to 7. Moreover, after 45 min, $H_2O_2$ concentration for pH 3 is higher than that for pH 1 or 2, respectively. Consequently, considering the consumption of acid and $H_2O_2$ concentration, pH 3 is determined as the most suitable pH condition.

The reasonable interpretations are as below. During the direct synthesis of hydrogen peroxide, the side reactions (Eqs. (2)–(4)) also occur together with the main synthesis reaction (Eq. (1)). For that, the acids are generally used as additives to improve the selectivity to hydrogen peroxide. It is reported that the acid additives can suppress

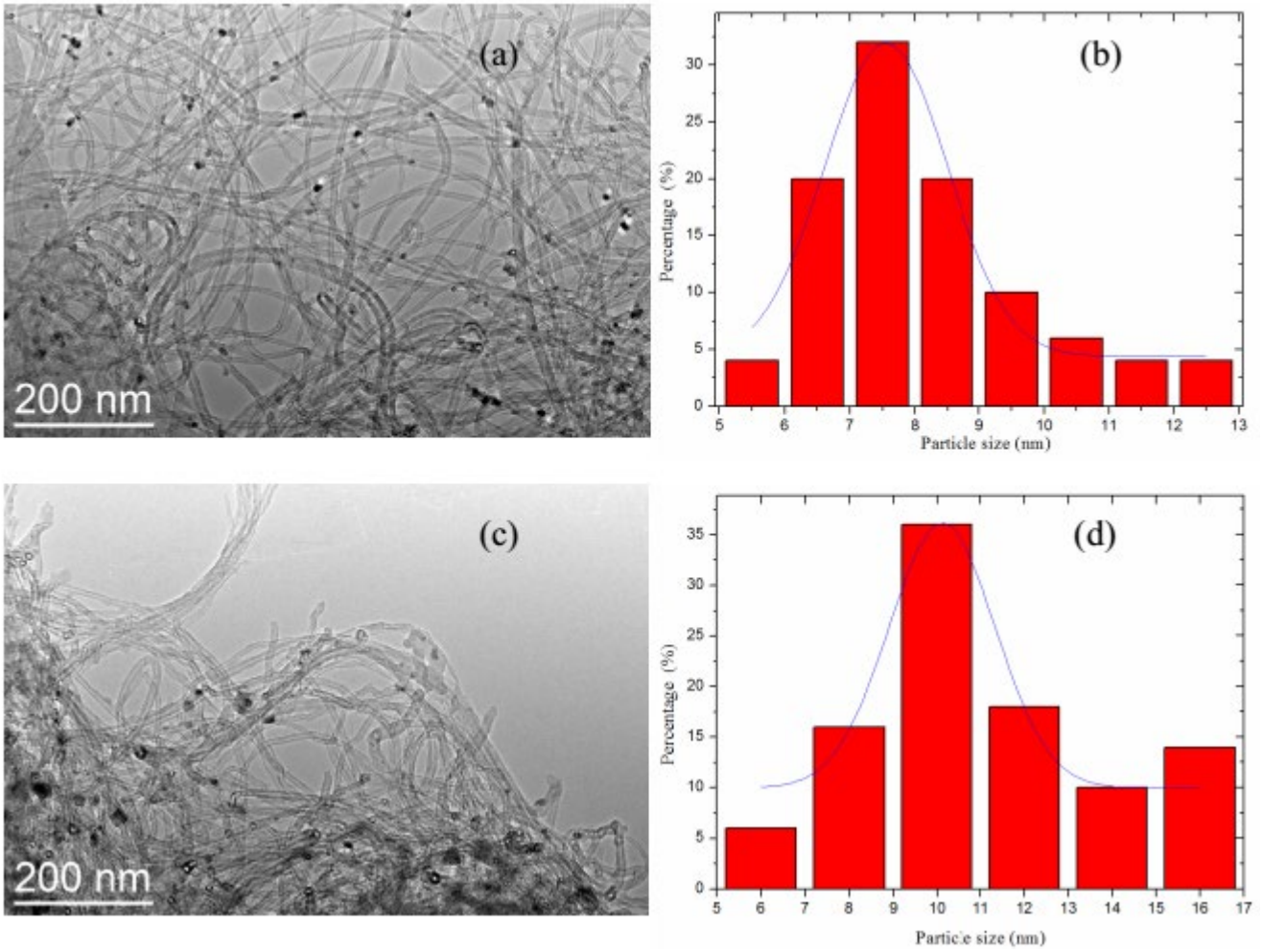


Fig. 2. TEM images (a and c) and corresponding particle size distribution histograms (b and d) of the fresh and used Pd/MWCNTs catalysts, respectively.

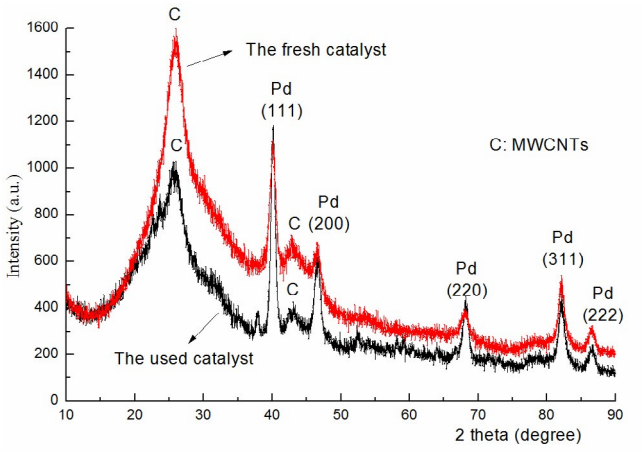


Fig. 3. XRD patterns of the fresh and used Pd/ MWCNTs catalysts.

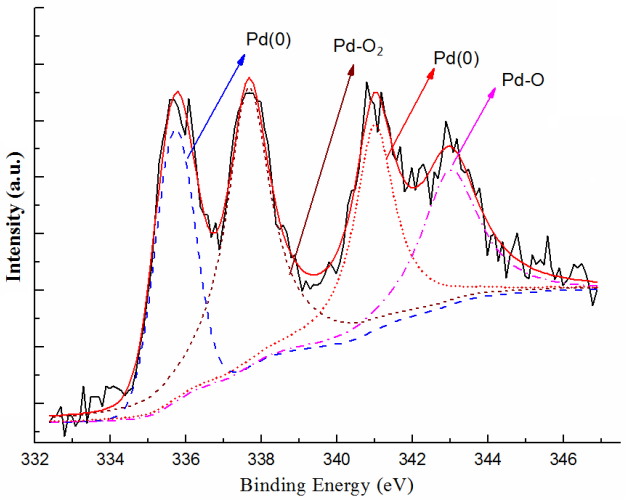


Fig. 4. XPS spectra of the fresh Pd/MWCNTs catalyst.

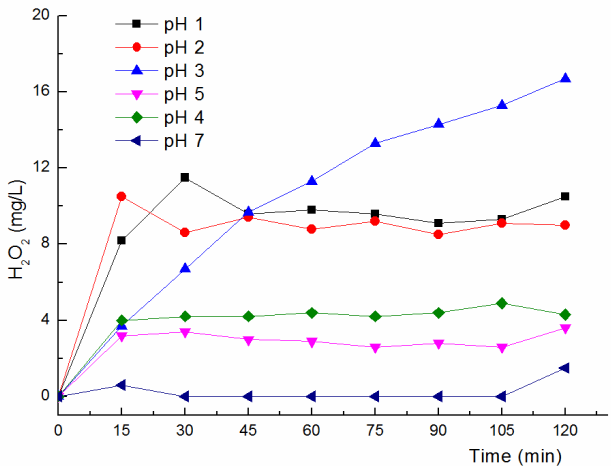


Fig. 5. Effect of pH on $H_2O_2$ concentration. Current density, 10 mA/cm²; voltage fluctuating range, 3.1–4.5 V; catalyst dosage, 0.5 g; interelectrode distance, 15 mm; agitation speed, 700 rpm.

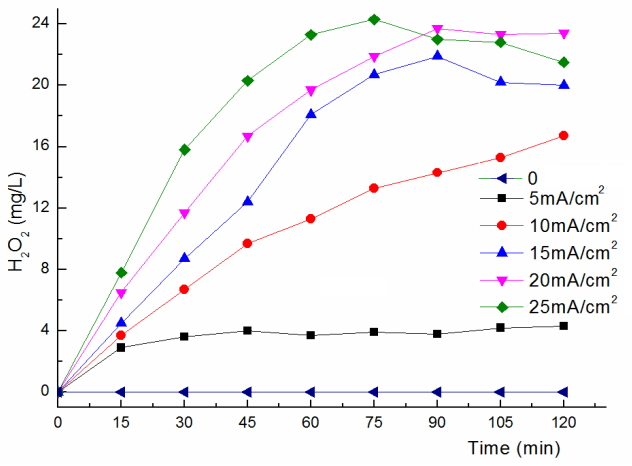


Fig. 6. Effect of current density on $H_2O_2$ concentration. pH, 3; voltage fluctuating range, 2.7–4.5 V; catalyst dosage, 0.5 g; interelectrode distance, 15 mm; agitation speed, 700 rpm.

the decomposition and hydrogenation reactions of hydrogen peroxide [1,4,16,17,20,22], which is the main reason that $H_2O_2$ concentrations decrease when pH rises from 3 to 7. However, excessive acid additives easily cause the dissolution of active noble metal component from the support materials for catalyst [4,17], as is a possible cause that after 45 min $H_2O_2$ concentration for pH 3 is higher than that for pH 1 or 2, respectively. And this is also a reason that $H_2O_2$ concentrations for pH 1 and 2 all climb rapidly to a top in 30 min and then slightly decrease.

### 3.2.2. Effect of current density

During water electrolysis, current density indicates the number of ions that are flowing through the electrolyte solution per unit time and cross-sectional area and affects the yield and emission rate of hydrogen and oxygen generated from water electrolysis [36]. The effect of current density on $H_2O_2$ concentration is demonstrated in Fig. 6.

As seen in Fig. 6, $H_2O_2$ concentrations for 5 and 10 mA/cm² all increase with time extending, and the concentration changing trend for 10 mA/cm² is more remarkable than that for 5 mA/cm². However, $H_2O_2$ concentrations for 15 and 20 mA/cm² increase rapidly in 90 min and then decrease slightly. Additionally, the concentration changing tendency for 25 mA/cm² is similar with those for 15 and 20 mA/cm². Significantly, $H_2O_2$ concentration is zero when the DC power is turned off, which suggests that $H_2O_2$ cannot be produced when Pd/MWCNTs catalyst is used only. Meantime, it can be also seen from Fig. 6 that at the same instant $H_2O_2$ concentrations sharply enhance in 75 min with current density rising from 5 to 25 mA/cm², and $H_2O_2$ concentration for 25 mA/cm² can get the highest value of 24 mg/L. Simultaneously, it is found that the β-$PbO_2$ film on the surface of anode easily flakes away in a tiny dot form when current density is 25 mA/cm². Hence, current density of 20 mA/cm² is applied in the subsequent experiments to extend service life of the Ti/β-$PbO_2$ anode.

During water electrolysis, the main reactions near the electrode surfaces are as follows:

Anodic reaction:

$$2H_2O - 4e^- \rightarrow O_2 + 4H^+ \quad (5)$$

Cathodic reaction:

$$2H_2O + 2e^- \rightarrow H_2 + 2OH^- \quad (6)$$

According to the Eqs. (5) and (6), the bigger current density is, the more hydrogen from the cathode and oxygen from the anode are. Thus, $H_2O_2$ concentration is the highest in accordance with the Eq. (1), which may be a main reason that $H_2O_2$ concentrations sharply enhance in 75 min with current density rising from 5 to 25 mA/cm². However, when $H_2O_2$ concentration becomes higher and higher, a small amount of hydrogen peroxide is decomposed, as may be a cause that $H_2O_2$ concentrations for 15, 20 and 25 mA/cm² attain to the top and then slightly decrease.

### 3.2.3. Effect of catalyst dosage

Catalyst dosage is a very important factor for in-situ synthesis of hydrogen peroxide and influences not only $H_2O_2$ concentration but also the cost of the adopted process. The effect of catalyst dosage on $H_2O_2$ concentration is illustrated in Fig. 7.

As shown in Fig. 7, under different catalyst dosage, $H_2O_2$ concentrations all increase with reactive time prolonging. Thereinto, $H_2O_2$ concentrations for 0.25, 0.5 and 1 g increase rapidly. Remarkably, $H_2O_2$ does not emerge when the DC power is supplied only. However, at the same instant, $H_2O_2$ concentrations initially improve with catalyst dosage rising from 0.25 to 0.5 g, and then gradually drop down when catalyst dosage ascending to 1.8 g. The results are consistent with literatures [13]. Meantime, the results also suggest that there is an optimal catalyst dosage when the dosage changes from 0.25 to 1.8 g. Therefore, 0.5 g is regarded as the optimum catalyst dosage and used in the future experiments.

The reasonable explanations are as follows. As current density of 20 mA/cm² keep stable, for different catalyst

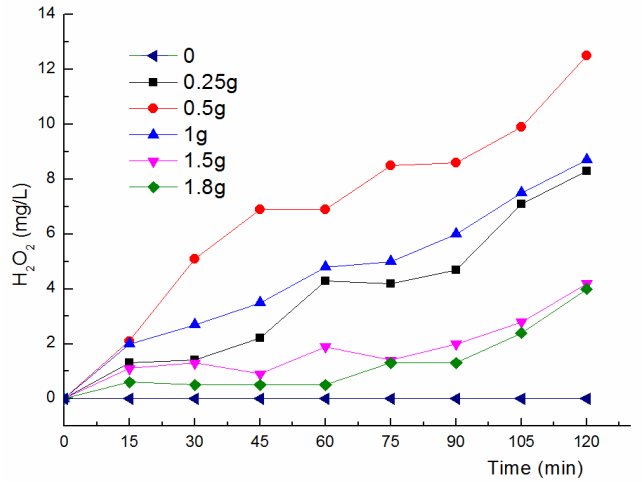


Fig. 7. Effect of catalyst dosage on $H_2O_2$ concentration. Current density, 20 mA/cm$^2$; voltage fluctuating range, 4.1~4.9 V; pH, 3; interelectrode distance, 15 mm; agitation speed, 700 rpm.

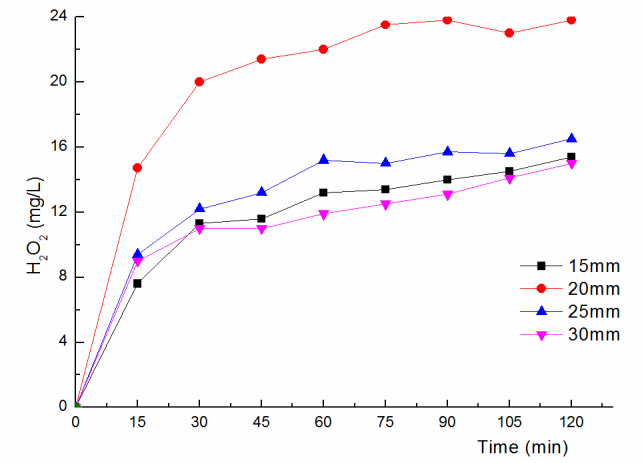


Fig. 8. Effect of interelectrode distance on $H_2O_2$ concentration. Current density, 20 mA/cm$^2$; voltage fluctuating range, 4.4~5.2 V; pH, 3; Catalyst dosage, 0.5 g; Agitation speed, 700 rpm.

dosage, the yield of hydrogen and oxygen generated from water electrolysis is also constant according to Eqs. (5) and (6). Accordingly, the more catalyst dosage is, the higher $H_2O_2$ concentration is, which is a reason that $H_2O_2$ concentrations improve with catalyst dosage rising from 0.25 to 0.5 g. However, when catalyst dosage is excessive, it is reported that the selectivity to $H_2O_2$ decreases rapidly and three side reactions, namely the oxidation of hydrogen with oxygen to form water, decomposition of $H_2O_2$ and the hydrogenation of hydrogen peroxide to form water (Eqs. (2)–(4)), are obvious [2,13,24], which is a reason that $H_2O_2$ concentrations gradually drop down when catalyst dosage ascends to 1.8 g.

### 3.2.4. *Effect of interelectrode distance*

As hydrogen and oxygen generated from water electrolysis are discharged from the electrode surfaces and dissolved into water, interelectrode distance affects the spatial distribution of hydrogen and oxygen in the reactor and further does $H_2O_2$ concentration. The effect of interelectrode distance on $H_2O_2$ concentration is presented in Fig. 8.

As seen from Fig. 8, $H_2O_2$ concentrations for different interelectrode distance all increase with time improving. Thereinto, $H_2O_2$ concentration for 20 mm improves strikingly. In addition, at the same instant, $H_2O_2$ concentrations increase dramatically when interelectrode distance changes from 15 to 20 mm. However, $H_2O_2$ concentrations decrease gradually while interelectrode distance continuously enhancing to 30 mm. The above results imply that there is an optimal interelectrode distance of 20 mm where the highest $H_2O_2$ concentration is gotten.

To explain the above results, Fig. 9 depicts the relations between the interelectrode distance and the diffusion area of oxygen and hydrogen. Except the interelectrode distance, the other experimental conditions are all uniform, and so it is reasonably assumed that the oxygen discharging speed from the anodic surface and the oxygen diffusing rate into water are constant. Thus, oxygen is diffused into the ring-shaped area near the surface of electrode (Fig. 9). The diffusion feature of

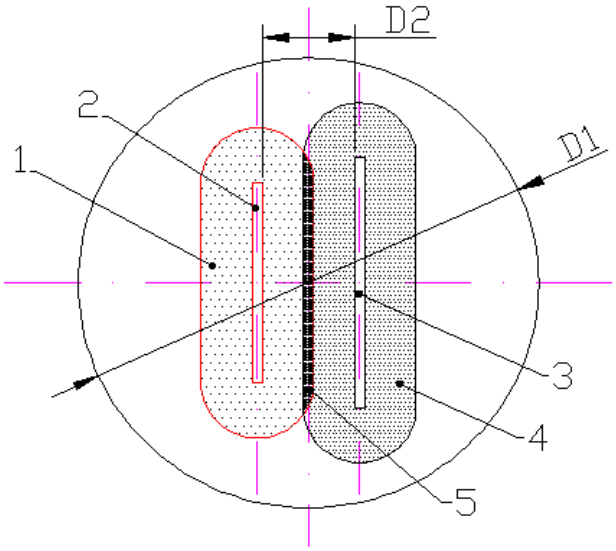


Fig. 9. Sectional view when the electrodes inserting into glass beaker. (1) Diffusion area of oxygen, (2) the anode, (3) the cathode, (4) diffusion area of hydrogen, (5) the overlap area of oxygen and hydrogen D1: The inner diameter (Φ = 45 mm) of the beaker D2: Distance between the electrodes.

hydrogen is similar with that of oxygen. Consequently, seen from Fig. 9, the interelectrode distance influences directly the effective diffusion area. For example, when the distance becomes small, the effective diffusion area reduces owing to the two diffusion areas overlapping. In addition, agitation speed of the solution between the two electrodes decreases due to interelectrode distance becoming small. Therefore, the catalyst between the two electrodes also reduces the collision chance to oxygen and hydrogen. Similarly, when the interelectrode distance exceeds the limit, the effective diffusion area also reduces due to narrow spaces between the electrodes and the inner wall of the beaker, and agitation speed of water between the narrow spaces also decreases. All these

have an impact on $H_2O_2$ concentration, which may be the main reasons for the above results.

### 3.2.5. Effect of agitation speed

The magnetic agitation speed dramatically affects the collision opportunity between oxygen, hydrogen and catalyst, and further influences on $H_2O_2$ concentration. Fig. 10 depicts the effect of agitation speed on $H_2O_2$ concentration.

As demonstrated in Fig. 10, when agitation speed changes from 230 to 1,050 rpm, $H_2O_2$ concentration for 230 rpm is the lowest and is about 16 mg/L in 120 min. Conversely, $H_2O_2$ concentration for 460 rpm is the highest and can attain to approximately 28 mg/L in 90 min. However, for agitation speed of 700 and 1,050 rpm, $H_2O_2$ concentration for 1,050 rpm is lower in 70 min than that for 700 rpm, and afterwards it is on the contrary. The results infer that 460 rpm is the most suitable agitation speed.

The reasonable explanations are as follows. For a given current, the yield of hydrogen and oxygen from water electrolysis is also constant according to Eqs. (5) and (6). At a lower agitation speed, the collision opportunity between oxygen, hydrogen and catalyst becomes less, and so $H_2O_2$ concentration goes lower. However, when agitation speed becomes higher, the catalyst has moved rapidly to the next space area before oxygen and hydrogen gets to the surface of catalyst, which makes the contacting opportunity between oxygen, hydrogen and catalyst less. Therefore, $H_2O_2$ concentration goes lower, too.

### 3.2.6. Effect of cations

Some ordinary cations, such as $K^+$, $Na^+$, $Ca^{2+}$ and $Mg^{2+}$, are often found in the surface water, and their existence affects possibly $H_2O_2$ concentration. For that, to get the simulated water containing $K^+$, $Na^+$, $Ca^{2+}$ and $Mg^{2+}$, $KNO_3$, $NaNO_3$, $Ca(NO_3)_2$ and $Mg(NO_3)_2$ (Analytical grade) are also added into distilled water according to the experimental requirements. According to the literatures [37,38], initial concentration of $K^+$, $Na^+$, $Ca^{2+}$ and $Mg^{2+}$ in solution is 20, 120, 98 and 22 mg/L, respectively. For solution containing four cations, the fore-mentioned water is mixed together. The effect of different cations on $H_2O_2$ concentration is estimated in Fig. 11.

As seen in Fig. 11, $H_2O_2$ concentration for no extra addition solution is the lowest and is about 28 mg/L in 90 min. As for water containing $Ca^{2+}$, its $H_2O_2$ concentration is only slightly higher than that for no extra addition water. Additionally, for water containing $K^+$ or $Na^+$, respectively, $H_2O_2$ concentrations are nearly equal and are all higher than the fore-mentioned water's. Remarkably, $H_2O_2$ concentration for solution including $Mg^{2+}$ is the highest and can rapidly get to about 36 mg/L in 30 min, which suggests that $Mg^{2+}$ ion is helpful to in-situ synthesis of hydrogen peroxide. However, $H_2O_2$ concentration for solution containing four cations is slightly higher than that for water containing $Ca^{2+}$. In addition, its $H_2O_2$ concentration is also lower than that for water containing $K^+$ or $Na^+$, respectively. For solution containing four cations, it seems that $Ca^{2+}$ ion plays a negative role in synthesizing hydrogen peroxide. However, the above results are worth further exploring.

### 3.3. Analysis on energy consumption

Energy consumption is one of the important indexes when the process is used for synthesis of hydrogen peroxide. Excess energy consumption will increase the operational cost and prevent the process from broadly spreading, too. Hence, energy consumption for different current density is analyzed as an example. During the calculations, energy ($E_m$), which is applied to produce a unit mass of hydrogen peroxide, is calculated by Eq. (7).

$$E_m = \frac{\int_0^t IVdt}{V_s C_t} \tag{7}$$

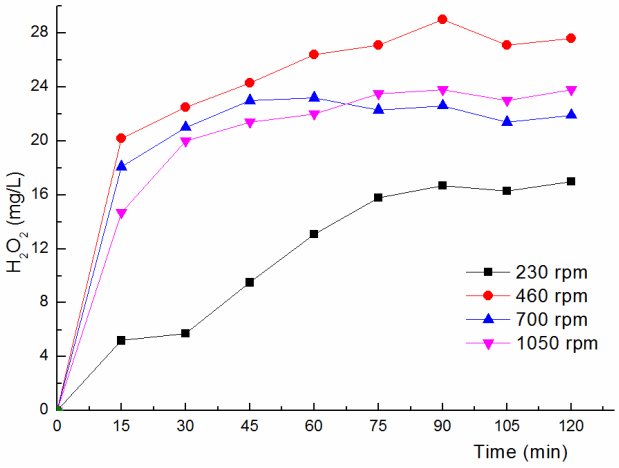


Fig. 10. Effect of agitation speed on $H_2O_2$ concentration. Current density, 20 mA/cm$^2$; voltage fluctuating range, 4.7–4.8 V; pH, 3; catalyst dosage, 0.5 g; interelectrode distance, 20 mm.

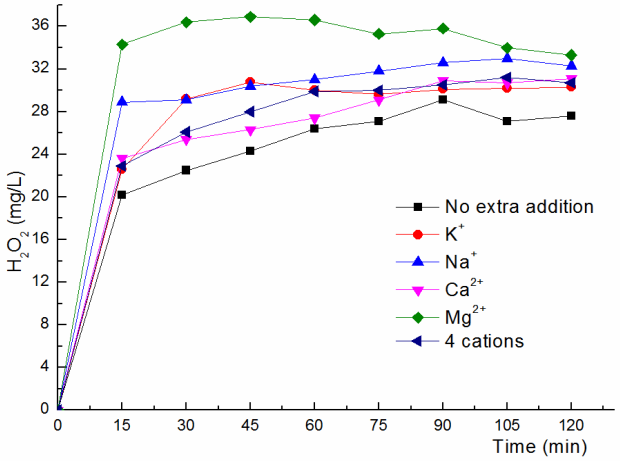


Fig. 11. Effect of different cations on $H_2O_2$ concentration. Current density, 20 mA/cm$^2$; voltage fluctuating range, 4.9–5.6 V; pH, 3; catalyst dosage, 0.5 g; Interelectrode distance, 20 mm; agitation speed, 460 rpm.

Table 1
Analysis on energy consumption for different current density

| Current density ($mA/cm^2$) | 5 | 10 | 15 | 20 | 25 |
|---|---|---|---|---|---|
| $E_m$ ($kWh\ kg^{-1}$) | 288.5 | 213.0 | 265.7 | 289.2 | 368.8 |

where $I$ is the current flown through the cathode and the anode (A), $V$ is the potential supplied to the two electrodes (V), $t$ is the reactive time (S), $V_S$ is the volume of the solution (L), $C_t$ is $H_2O_2$ concentration (mg/L) at $t$ moment.

According to the results from Fig. 6, $H_2O_2$ concentrations for different current density all show an increasing tendency in 75 min, and so during the calculations 75 min is regarded as an effective time. According to Eq. (7), energy consumption for different current density is listed in Table 1. The table demonstrates that when current density varies from 10 to 25 $mA/cm^2$, $E_m$ increases from 213.0 to 368.8 kWh/kg, which implies that energy consumption sharply enhances. However, for the lowest current density of 5 $mA/cm^2$, its $E_m$ is 288.5 kWh/kg and energy consumption is very high, too. All these results suggest that there lies the optimal current density of 10 $mA/cm^2$ where energy consumption is the smallest [39,40].

## 4. Conclusions

In this paper, the ordinary Ti/β-$PbO_2$ anode and graphite cathode are used to construct the water electrolysis system. In-situ synthesis of hydrogen peroxide using water electrolysis and Pd/MWCNTs catalyst is investigated. Some conclusions can be drawn as below.

The results from TEM/EDS, XRD and XPS show the distribution and crystal structure of Pd on MWCNTs.

The optimal experimental conditions, which are current density of 20 $mA/cm^2$, pH of 3, catalyst dosage of 0.5 g, interelectrode distance of 20 mm and agitation speed of 460 rpm, are determined and its $H_2O_2$ concentration can attain to about 28 mg/L in 90 min. Additionally, under the above conditions, $H_2O_2$ concentration for water including $Mg^{2+}$ ion can rapidly get to about 36 mg/L in 30 min. $E_m$ increases from 213.0 to 368.8 kWh/kg when current density varying from 10 to 25 $mA/cm^2$. However, for the lowest current density of 5 $mA/cm^2$, its $E_m$ is 288.5 kWh/kg and is very high, too.

In-situ synthesis of hydrogen peroxide using water electrolysis and Pd/MWCNTs catalyst is feasible.

## Acknowledgments

This work was supported by Hubei Provincial Natural Science Foundation of China (No. 2016CFB588) and Hubei Key Laboratory of Animal Nutrition and Feed Science, Wuhan Polytechnic University (No. 201911).

## References

[1] R. Dittmeyer, J.-D. Grunwaldt, A. Pashkova, A review of catalyst performance and novel reaction engineering concepts in direct synthesis of hydrogen peroxide, Catal. Today, 248 (2015) 149–159.
[2] V. Paunovic, J.C. Schouten, T.A. Nijhuis, Direct synthesis of hydrogen peroxide using concentrated $H_2$ and $O_2$ mixtures in a wall-coated microchannel – kinetic study, Appl. Catal., A, 505 (2015) 249–259.
[3] M.-g. Seo, S. Kim, D.-W. Lee, H.E. Jeong, K.-Y. Lee, Core–shell structured, nano-Pd-embedded $SiO_2$–$Al_2O_3$ catalyst (Pd@SiO2–Al2O3) for direct hydrogen peroxide synthesis from hydrogen and oxygen, Appl. Catal., A, 511 (2016) 87–94.
[4] S. Park, J. Lee, J.H. Song, T.J. Kim, Y.-M. Chung, S.-H. Oh, I.K. Song, cM-5 catalysts: effect of Brönsted acidity, J. Mol. Catal., A, 363–364 (2012) 230–236.
[5] E. Pizzutilo, O. Kasian, C.H. Choi, S. Cherevko, G.J. Hutchings, K.J.J. Mayrhofer, S.J. Freakley, Electrocatalytic synthesis of hydrogen peroxide on Au-Pd nanoparticles: from fundamentals to continuous production, Chem. Phys. Lett., 683 (2017) 436–442.
[6] D. Gudarzi, W. Ratchananusorn, I. Turunen, T. Salmi, M. Heinonen, Preparation and study of Pd catalysts supported on activated carbon cloth (ACC) for direct synthesis of $H_2O_2$ from H2 and O2, Top. Catal., 56 (2013) 527–539.
[7] B. Hu, W. Deng, R. Li, Q. Zhang, Y. Wang, F. Delplanque-Janssens, D. Paul, F. Desmedt, P. Miquel, Carbon-supported palladium catalysts for the direct synthesis of hydrogen peroxide from hydrogen and oxygen, J. Catal., 319 (2014) 15–26.
[8] C. Samanta, Direct synthesis of hydrogen peroxide from hydrogen and oxygen: an overview of recent developments in the process, Appl. Catal., 350 (2008) 133–149.
[9] F. Menegazzo, M. Signoretto, M. Manzoli, F. Boccuzzi, G. Cruciani, F. Pinna, G. Strukul, Influence of the preparation method on the morphological and composition properties of Pd–Au/$ZrO_2$ catalysts and their effect on the direct synthesis of hydrogen peroxide from hydrogen and oxygen, J. Catal., 268 (2009) 122–130.
[10] V. Paunovic, J.C. Schouten, T.A. Nijhuis, Direct synthesis of hydrogen peroxide in a wall-coated microchannel reactor over Au–Pd catalyst: a performance study, Catal. Today, 248 (2015) 160–168.
[11] T. Inoue, J. Adachi, K. Ohtaki, M. Lu, S. Murakami, X. Sun, D.F. Wang, Direct hydrogen peroxide synthesis using glass microfabricated reactor – paralleled packed bed operation, Chem. Eng. J., 278 (2015) 517–526.
[12] J.W. Lee, J.K. Kim, T.H. Kang, E.J. Lee, I.K. Song, Direct synthesis of hydrogen peroxide from hydrogen and oxygen over palladium catalyst supported on heteropolyacid-containing ordered mesoporous carbon, Catal. Today, 293–294 (2017) 49–55.
[13] W. Ratchananusorn, D. Gudarzi, I. Turunen, Catalytic direct synthesis of hydrogen peroxide in a novel microstructured reactor, Chem. Eng. Process., 84 (2014) 24–30.
[14] M.S. Yalfani, S. Contreras, F. Medina, J.E. Sueiras, Hydrogen substitutes for the in situ generation of $H_2O_2$: an application in the Fenton reaction, J. Hazard. Mater., 192 (2011) 340–346.
[15] B. Puértolas, A.K. Hill, T. García, B. Solsona, L. Torrente-Murciano, In-situ synthesis of hydrogen peroxide in tandem with selective oxidation reactions: a mini-review, Catal. Today, 248 (2015) 115–127.
[16] J.K. Edwards, J. Pritchard, P.J. Miedziak, M. Piccinini, A.F. Carley, Q. He, C.J. Kiely, G.J. Hutchings, The direct synthesis of hydrogen peroxide using platinum promoted gold–palladium catalysts, Catal. Sci. Technol., 4 (2014) 3244–3250.
[17] J.K. Edwards, S.J. Freakley, R.J. Lewis, J.C. Pritchard, G.J. Hutchings, Advances in the direct synthesis of hydrogen peroxide from hydrogen and oxygen, Catal. Today, 248 (2015) 3–9.
[18] S.J. Freakley, Q. He, J.H. Harrhy, L. Lu, D.A. Crole, D.J. Morgan, E.N. Ntainjua, J.K. Edwards, A.F. Carley, A.Y. Borisevich, C.J. Kiely, G.J. Hutchings, Palladium-tin catalysts for the direct synthesis of $H_2O_2$ with high selectivity, Science, 6276 (2016) 965–968.
[19] M.S. Yalfani, S. Contreras, F. Medina, J. Sueiras, Phenol degradation by Fenton's process using catalytic in situ generated hydrogen peroxide, Appl. Catal., B, 89 (2009) 519–526.
[20] S. Yuan, Y. Fan, Y. Zhang, M. Tong, P. Liao, Pd-catalytic in situ generation of $H_2O_2$ from $H_2$ and $O_2$ produced by water

electrolysis for the efficient electro-Fenton degradation of Rhodamine B, Environ. Sci. Technol., 45 (2011) 8514–8520.
[21] S. Park, J.H. Choi, T.J. Kim, Y.-M. Chung, S.-H. Oh, I.K. Song, Direct synthesis of hydrogen peroxide from hydrogen and oxygen over Pd/CsXH3-XPW12O40/MCF (X = 1.7, 2.0, 2.2, 2.5, and 2.7) catalysts, J. Mol. Catal., A, 353–354 (2012) 37–43.
[22] M.-g. Seo, S. Kim, H.E. Jeong, D.-W. Lee, K.-Y. Lee, A yolk–shell structured Pd@void@$ZrO_2$ catalyst for direct synthesis of hydrogen peroxide from hydrogen and oxygen, J. Mol. Catal., A, 413 (2016) 1–6.
[23] V.R. Choudhary, A.G. Gaikwad, S.D. Sansare, Activation of supported Pd metal catalysts for selective oxidation of hydrogen to hydrogen peroxide, Catal. Lett., 83 (2002) 235–239.
[24] S. Fan, J. Yi, L. Wang, Z. Mi, Direct synthesis of hydrogen peroxide from $H_2/O_2$ using $Pd/Al_2O_3$ catalysts, React. Kinet. Catal. Lett., 92 (2007) 175–182.
[25] H.E. Jeong, S. Kim, M.-g. Seo, D.-W. Lee, K.-Y. Lee, Catalytic activity of Pd octahedrons/$SiO_2$ for the direct synthesis of hydrogen peroxide from hydrogen and oxygen, J. Mol. Catal., A, 420 (2016) 88–95.
[26] S. Kim, D.-W. Lee, K.-Y. Lee, Shape-dependent catalytic activity of palladium nanoparticles for the direct synthesis of hydrogen peroxide from hydrogen and oxygen, J. Mol. Catal., A, 391 (2014) 48–54.
[27] J.M. Aquino, R.C. Rocha-Filho, L.A.M. Ruotolo, N. Bocchi, S.R. Biaggio, Electrochemical degradation of a real textile wastewater using β-$PbO_2$ and DSAR anodes, Chem. Eng. J., 251 (2014) 138–145.
[28] J.M. Aquino, R.C. Rocha-Filho, N. Bocchi, S.R. Biaggio, Electrochemical degradation of the Reactive Red 141 dye on a β-PbO2 anode assessed by the response surface methodology, J. Braz. Chem. Soc., 21 (2010) 324–330.
[29] H. Zhang, Y.A. Alhamed, W. Chu, Z. Ye, A. AlZahrani, L. Petrov, Controlling Co-support interaction in Co/MWCNTs catalysts and catalytic performance for hydrogen production via NH3 decomposition, Appl. Catal., A, 464–465 (2013) 156–164.
[30] J. Yuan, Y. Zhu, Y. Li, L. Zhang, L. Li, Effect of multi-wall carbon nanotubes supported palladium addition on hydrogen storage properties of magnesium hydride, Int. J. Hydrogen Energy, 39 (2014) 10184–10194.
[31] O. Arciniega Cano, C.A. Rodríguez González, J.F. Hernández Paz, P. Amezaga Madrid, P.E. García Casillas, A.L. Martínez Hernández, C.A. Martínez Pérez, Catalytic activity of palladium nanocubes/multiwalled carbon nanotubes structures for methyl orange dye removal, Catal. Today, 282 (2017) 168–173.
[32] K. Wu, X. Mao, Y. Liang, Y. Chen, Y. Tang, Y. Zhou, J. Lin, C. Ma, T. Lu, Multiwalled carbon nanotubes supported palladium ephosphorus nanoparticles for ethanol electrooxidation in alkaline solution, J. Power Sources, 219 (2012) 258–262.
[33] K. Ding, Y. Zhao, L. Liu, Y. Li, L. Liu, Y. Wang, H. Gu, H. Wei, Z. Guo, Multi-walled carbon nanotubes supported Pd composite nanoparticles hydrothermally produced from technical grade PdO precursor, Electrochim. Acta, 176 (2015) 1256–1265.
[34] H. An, H. Cui, D. Zhou, D. Tao, B. Li, J. Zhai, Q. Li, Synthesis and performance of Pd/$SnO_2$–$TiO_2$/MWCNT catalysts for direct formic acid fuel cell application, Electrochim. Acta, 92 (2013) 176–182.
[35] B. Lesiak, M. Mazurkiewicz, A. Malolepszy, L. Stobinski, B. Mierzwa, A. Mikolajczuk-Zychora, K. Juchniewicz, A. Borodzinski, J. Zemek, P. Jiricek, Effect of the Pd/MWCNTs anode catalysts preparation methods on their morphology and activity in a direct formic acid fuel cell, Appl. Surf. Sci., 387 (2016) 929–937.
[36] M. Majlesi, S.M. Mohseny, M. Sardar, S. Golmohammadi, A. Sheikhmohammadi, Improvement of aqueous nitrate removal by using continuous electrocoagulation/electroflotation unit with vertical monopolar electrodes, Sustain. Environ. Res., 26 (2016) 287–290.
[37] D. Fu, X. Wang, J. Liu, A. Zhang, The investigate and analysis about background value of water environmental in the soure area of Yangtze River (In Chinese), Environ. Mon. in China, 14 (1998) 9–11.
[38] X. He, Y. Wu, J. Zhou, H. Bing, Hydro-chemical characteristics and quality assessment of surface water in Gongga Mountain region (in Chinese), Environ. Sci., 37 (2016) 3798–3805.
[39] A. Sheikhmohammadi, A. Yazdanbakhsh, G. Moussavi, A. Eslami, M. Rafiee, M. Sardar, M. Almasian, Degradation and COD removal of trichlorophenol from wastewater using sulfite anion radicals in a photochemical process combined with a biological reactor: mechanisms, degradation pathway, optimization and energy consumption, Process Saf. Environ., 123 (2019) 263–271.
[40] H. Godini, A. Sheikhmohammadi, L. Abbaspour, R. Heydari, G.S. Khorramabadi, M. Sardar, Z. Mahmoudi, Energy consumption and photochemical degradation of Imipenem/Cilastatin antibiotic by process of UVC/$Fe^{2+}$/$H_2O_2$ through response surface methodology, Optik, 182 (2019) 1194–1203.